Korean J. Chem. Eng., 34(5), 1337-1345 (2017)
DOI: 10.1007/s11814-017-0020-6

pISSN: 0256-1115
eISSN: 1975-7220

Effect of Cu promoter and alumina phases on Pt/Al_2O_3 for propane dehydrogenation

Hakbeum Lee*, Won-Il Kim, Kwang-Deog Jung***, and Hyoung Lim Koh*,†**

*Department of Chemical Engineering, RCCT, Hankyong National University, Anseong 17579, Korea
**Hyosung R&D Labs., 74 Simin-daero, Dongan-gu, Anyang-si, Gyunggi-do 431-080, Korea
***Clean Energy Research Center, Korea Institute of Science and Technology,
Cheongryang, P. O. Box 131, Seoul 02792, Korea
(*Received 6 September 2016 • accepted 6 February 2017*)

Abstract−We investigated the effects of different Cu weight ratio on θ or γ-Al_2O_3 which were impregnated with platinum in terms of catalytic activity for propane dehydrogenation and physicochemical properties. 1.5 wt% Pt, 0-10 wt% Cu catalyst supported on θ-Al_2O_3 or γ-Al_2O_3 was prepared by incipient wetness co-impregnation. Enhanced Pt dispersion by increasing Cu contents in γ-Al_2O_3 supported catalyst was confirmed via XRD and XPS. Pt and CuO was separated in Pt-Cu/θ-Al_2O_3, but Pt-Cu alloy was identified after reduction treatment. Also, adding Cu in Pt/Al_2O_3 makes catalyst's acidity lower and this property led to increased propylene yield in propane dehydrogenation. However, Pt_3Cu was not good for yield of PDH, which was confirmed in Pt-10Cu/θ-Al_2O_3 through XRD.

Keywords: Propane Dehydrogenation, Platinum, Copper, Acidity, Alumina

INTRODUCTION

Propylene, alongside ethylene, is one of the most useful light olefins, as it is used for producing various petrochemicals such as polypropylene, propylene oxide and acrylic acid [1-4]. High demand for propylene has led to an interest in development of processes, which is the main product, and not a byproduct, such as in steam cracking of naphtha and fluidized catalytic cracking [5,6]. Among the commercial processes, propane dehydrogenation is not only widely used in chemical industries and has received significant attention, but also has been studied to have positive possibility as a propylene manufacture [7]. The corresponding chemical reaction is:

$$C_3H_8 \leftrightarrow C_3H_6+H_2 \quad \Delta H_f^o=124\ kJmol^{-1} \tag{1}$$

It is not only an endothermic and equilibrium limited reaction, but also requires a low pressure and a high reaction temperature 550-620 °C to achieve a high propylene yield [8]. Al_2O_3 supported Pt catalysts are commonly used in industrial dehydrogenation processes. However, the selectivity is not as high as desired due to generation of lighter hydrocarbons through C-C bond cleavage [9], and occurrence of side reactions such as cracking and hydrogenolysis [10]. Bimetallic catalysts, with platinum as the primary metal and a second metal (e.g., Sn, Cu, Re, Ir, and Cs) as a promoter, have been studied extensively [11,12].

Cu has also been considered as a second metal for Pt as a catalyst in naphtha reforming [13], alcohol dehydrogenation [14] and electrochemistry [15-17]. It is known that in Pt-Cu bimetallic catalysts [18], Cu can dissolve Pt metal particles, bring about an increase in dispersion and decrease in ensemble size [19]. In naphtha reforming, addition of Cu to Pt catalyst can increase cracking or hydrogenolysis [20]. This suggests that if a bimetallic Pt-Cu catalyst is employed in propane dehydrogenation, the decrease in selectivity for propylene will need to be compensated by using another method, such as change or modification of the alumina (Al_2O_3) support, to increase yield to propylene.

In this study, we prepared Pt-Cu/Al_2O_3 catalysts with varying Cu content and different phases of Al_2O_3, and compared their catalytic performance for propane dehydrogenation. Furthermore, we investigated the effect of increasing Cu content, on Pt dispersion and formation of coke on the surface of spent catalyst. The catalysts were characterized using N_2 adsorption (BET), thermogravimetric analysis (TGA), Raman spectroscopy, X-ray diffraction (XRD), X-Ray photoelectron spectroscopy (XPS), transmission electronic microscopy (TEM) and NH_3-TPD. Finally, we analyzed the correlation between changes in the properties and activities of the catalysts.

EXPERIMENTAL

1. Catalyst Preparation

$H_2PtCl_6 \cdot 5.5H_2O$ (Kojima) and $Cu(NO_3)_2 \cdot 3H_2O$ (Daejung) were used as metal precursors in supported Pt-Cu catalysts. $H_2PtCl_6 \cdot 5.5H_2O$ and $Cu(NO_3)_2 \cdot 3H_2O$ dissolved in distilled water were co-impregnated with γ or θ-Al_2O_3 (γ-Al_2O_3 Support was supplied by SASOL and θ-Al_2O_3 support was prepared by calcining the spherical γ-Al_2O_3 at 1,273 K for 6 h). Each sample was dried at 120 °C for 12 h and then calcined at 600 °C for 4 h.

2. Catalytic Activity Measurements

The catalytic activity of the catalysts for propane dehydrogenation was measured in a fixed-bed quartz reactor (inner diameter 18 mm) using 100 mg of each catalyst (grain size about 425 μm-

†To whom correspondence should be addressed.
E-mail: hlkoh@hknu.ac.kr

850 μm). The propane dehydrogenation reaction was performed at atmospheric pressure and 600 °C. A heating rate of 10 °C/min was applied up to 600 °C with H_2 (10 ml/min) and N_2 (40 ml/min) and then maintained for 1 h to stabilize the temperature. The reaction mixture composed of N_2 (10 ml/min), C_3H_8 (10 ml/min), and H_2 (10 ml/min) was fed into the reactor. The product was sampled at different intervals and analyzed by gas chromatography (FID detector, 5890 series2 plus, Hewlett Packard, USA). A 50 m× 0.53 mm GS-Alumina capillary column was used.

Propane conversion, propylene selectivity, and propylene yield were calculated by the following equations:

$$\text{Propane conversion (\%)} = \left[1 - \frac{n(C_3H_8)_{out}}{n(C_3H_8 + C_3H_6 + C_2H_6 + C_2H_4 + CH_4)}\right] \times 100 \quad (2)$$

$$\text{Propylene selectivity (\%)} = \frac{n(C_3H_6)_{out}}{n(C_3H_6 + C_2H_6 + C_2H_4 + CH_4)} \times 100 \quad (3)$$

$$\text{Propylene yield (\%)} = \frac{\text{Propane conversion} \times \text{Propylene selectivity}}{100} \quad (4)$$

where, $n(C_3H_8)_{out}$ is the number of moles of propane at the outlet, and $n(CH_4)$, $n(C_2H_6)$, $n(C_2H_4)$, and $n(C_3H_6)$ are the number of moles of methane, ethane, ethylene, and propylene, respectively, at the outlet.

3. Characterization

The surface areas and pore size distributions of the catalysts were characterized by a nitrogen sorption technique (Belsorp-II mini, BEL Japan. Inc.). The samples were analyzed at −196 °C using an automatic gas system. The coke content was determined by a thermogravimetric analyzer (Pyris, PerkinElmer, USA). Approximately 10 mg of spent catalyst was charged into the sample pan and heated to 800 °C at a rate of 10 °C/min in flowing oxygen (20 ml/min). XRD patterns were measured by using a D/MAX-2500/PC X-ray diffractometer (Rigaku, Japan) with Cu Kα radiation. The X-ray tube was operated at 40 kV, and 200 mA. The 2θ angle was scanned from 20° to 80° at a scanning speed of 3°/min. Raman spectra were obtained at room temperature under ambient conditions using Renishaw in Via Raman microscope with a 532 nm Ar laser beam. TEM (JEM-2010, JEOL, Japan) was used for looking Pt dispersion comparing with XRD data. The exposure time and spectral range were 10 s and 800-2,200 cm^{-1}, respectively. The acidity of the samples was investigated by TPD of ammonia.

The experiments were conducted in a gas flow system, equipped with a quadrupole mass analyzer (Omni StarTM, Pfeiffer), using a U-shaped quartz reactor. The catalytic samples (0.09 g) were first pretreated under He flow (50 ml/min) for 1 h at 150 °C and then cooled to room temperature. Next, the samples were saturated with mixture gas (50 ml/min) of NH_3/He (15%) 80 °C for 1 h. Finally, TPD was performed by heating the sample to 800 °C under He (5 ml/min). XPS spectra were obtained with an AXIS NOVA spectrometer (KRATOS, England) equipped with a monochromatic electro analyzer and a monochromatic Al-Kα 150 W X-ray source. In addition to a binding energy scan range from 82 to 68 eV for the identification of all detectable elements, detailed scans for the chemical state identification and quantification were obtained.

RESULTS AND DISCUSSION

1. Characterization

Table 1 lists the surface areas, pore sizes and pore volumes of Pt-Cu/γ and θ-Al_2O_3 catalysts with different Cu content. The coke content on the surface of the spent catalysts is also shown in the table. Surface area of γ-Al_2O_3 supported catalysts is much higher than θ-Al_2O_3 supported catalysts because of the properties of γ and θ-Al_2O_3. As expected, the BET surface area of Al_2O_3 decreased on impregnation with Cu. Also, pore volume was decreased with increasing copper content. The amount of coke deposited on the Pt-*x*Cu/γ-Al_2O_3 catalysts after propane dehydrogenation for 5 h was obtained by TGA as 13.2, 16.5, 13.4, and 11.5% for x=0, 0.5, 5, and 10, respectively. In the case of θ-Al_2O_3 supported catalysts, the corresponding values of coke content were 8.6, 10.6, 8.8, and 5.2%, respectively. The formation of coke on a Pt-Cu/γ or θ-Al_2O_3 catalyst was similar or slightly lower than that on an analogous Pt/γ or θ-Al_2O_3. However, interestingly, coke content increased on Pt-0.5Cu/γ and θ-Al_2O_3. In the catalytic activity session in this paper, adding lower content of Cu has a role with increasing acid site which can generate the coke. Also, coke content of catalysts with γ-Al_2O_3 as support was higher than with θ-Al_2O_3 as support, because γ-Al_2O_3 has more acid sites than θ-Al_2O_3; lower acid sites interrupt the formation of coke [21]. Therefore, choosing the copper content in the catalysts works an important factor in the restraint of the generation of coke, and we can confirm that quantity of coke was related with catalytic acid and reaction activity.

Fig. 1 shows the results of the TGA of Pt-*x*Cu/γ and θ-Al_2O_3. At the Pt/γ-Al_2O_3 and Pt/θ-Al_2O_3, the weight loss started slowly at

Table 1. BET surface areas, pore diameters, and pore volumes obtained from N_2 physisorption and coke content in the spent catalysts

Catalyst	Surface area (m^2/g)	Pore volume (cm^3/g)	Pore size (nm)	Coke contents (%)
Pt/γ-Al_2O_3	207	0.53	6.81	13.168
Pt-0.5Cu/γ-Al_2O_3	196	0.53	4.08	16.523
Pt-5Cu/γ-Al_2O_3	166	0.47	4.51	13.425
Pt-10Cu/γ-Al_2O_3	122	0.32	4.09	11.49
Pt/θ-Al_2O_3	90	0.34	8.53	8.559
Pt-0.5Cu/θ-Al_2O_3	89	0.33	6.46	10.643
Pt-5Cu/θ-Al_2O_3	91	0.33	5.71	8.832
Pt-10Cu/θ-Al_2O_3	75	0.28	8.53	5.165

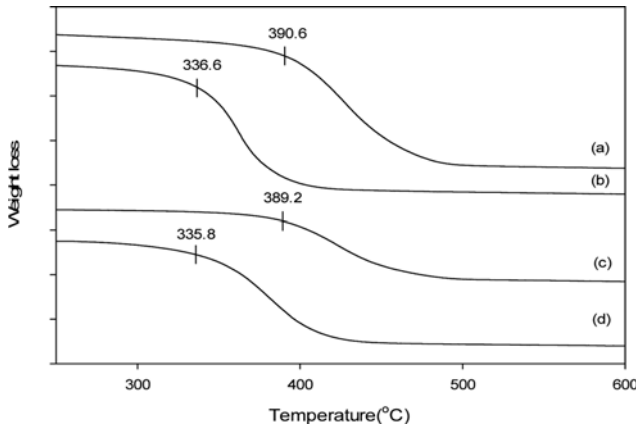

Fig. 1. TGA analysis with spent (a) Pt/γ-Al_2O_3, (b) Pt-5Cu/γ-Al_2O_3, (c) Pt/θ-Al_2O_3, (d) Pt-5Cu/θ-Al_2O_3 catalyst (O_2=20 ml/min, heating temperature: 10 °C/min).

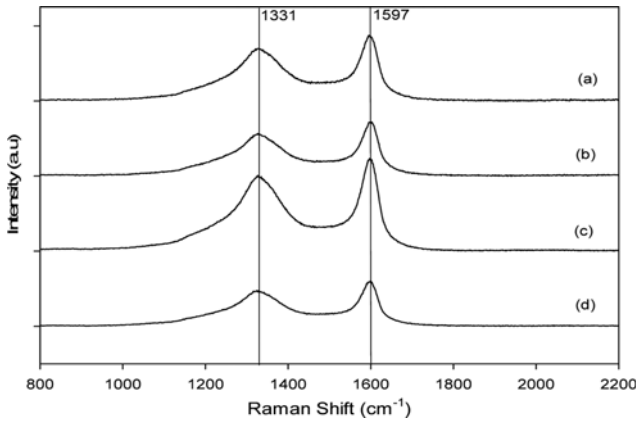

Fig. 2. Raman spectra of the spent catalysts after the dehydrogenation of propane has progressed for 5 h at 600 °C, (a) Pt/γ-Al_2O_3, (b) Pt-5Cu/γ-Al_2O_3, (c) Pt/θ-Al_2O_3, (d) Pt-5Cu/θ-Al_2O_3.

390.6 °C and 389.2 °C up to 500 °C, respectively. The weight of used Pt-5Cu/γ and θ-Al_2O_3 catalysts decreased at 336.6 °C and 335.8 °C, respectively. It means adding copper let the coke of Pt/Al_2O_3 catalyst decompose easily at low temperature as well as having an advantage for regeneration of catalysts.

Raman spectroscopy is a fast and nondestructive method for the characterization of carbon materials. Raman spectra of spent Pt/Al_2O_3 and Pt-Cu/Al_2O_3 catalysts were measured to examine the degree of graphitization of the formation of coke during propane dehydrogenation. As can be seen from Fig. 2, two distinct Raman bands are observed at 1,331 and 1,597 cm^{-1}, labeled D and G, respectively, which can be attributed to the C-H bending and C=C stretching in aromatic and alkyl hydrocarbons. Specifically, the G peak is due to the bond stretching of any pairs of sp^2 sites, while the D peak is caused by the breathing modes of sp^2 atoms in rings [22]. A high value of I_D/I_G implies lower graphitization of the carbon material [23]. The I_D/I_G values, that is, the intensity ratio of the D and G peaks to monitor carbon bonding of Pt/Γ-Al_2O_3, Pt-0.5Cu/Γ-Al_2O_3, Pt/θ-Al_2O_3 and Pt-0.5Cu/θ-Al_2O_3, are 0.71, 0.74, 0.69 and 0.69, respectively. Clearly, graphitization decreased on addition of Cu to Pt/γ and θ, from which it can be inferred that not only was coke oxidation in these materials simple, but also the coke oxidation temperature was lower and the coke formed was oxidized easily. Therefore, adding Cu could lead to facile regeneration of the catalysts.

Fig. 3 shows the XRD patterns of calcined Pt/Al_2O_3 and Pt-Cu/Al_2O_3 catalysts with different alumina phase. The Pt metal phase can be identified in all of catalysts by the characteristic peaks at 2θ=39.76, 46.24, and 67.45° (JCPDS card no. 04-0802). The γ and θ phases of Al_2O_3 were also detected in the calcined catalysts (JCPDS card no. 00-023-1009, 48-1548). It is noticeable from the figures that Pt/γ-Al_2O_3 exhibits the Pt peak at 2θ due to the crystalline of platinum. As the Pt peak disappears as the Cu content increases in Pt-Cu/γ-Al_2O_3, it means that Cu can be related with Pt dispersion. However, dispersion change of Pt in Pt-Cu/θ-Al_2O_3 was not observed. Thus, in regard to dispersion, Cu plays a more important

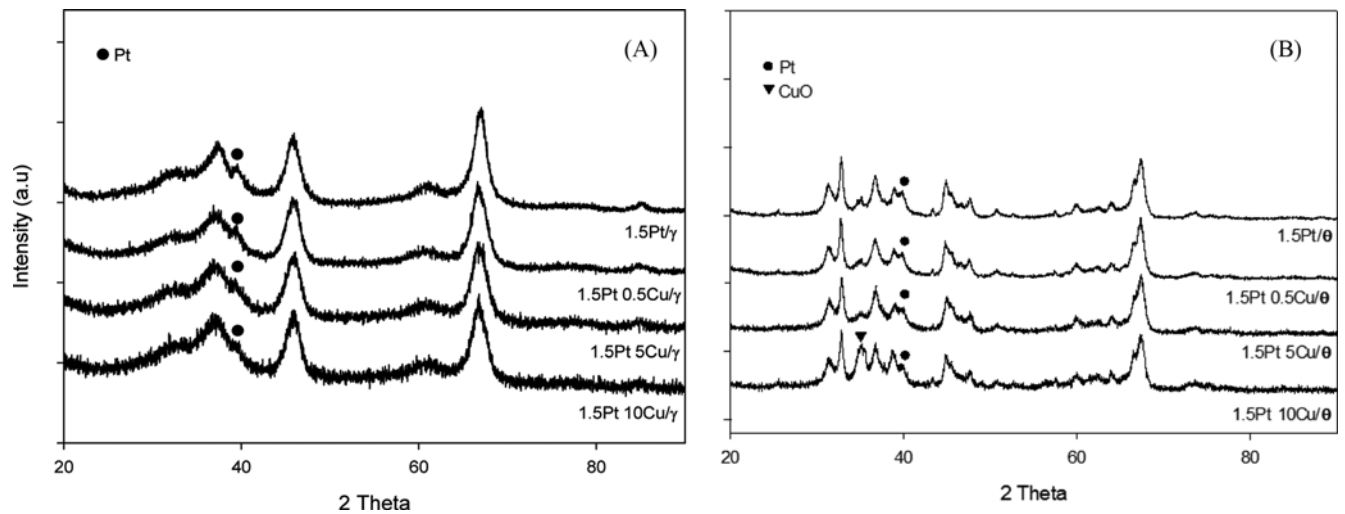

Fig. 3. XRD patterns of the Pt-Cu/Al_2O_3 catalysts with different copper contents and type of alumina as (A): (a) Pt/γ-Al_2O_3, (b) Pt-0.5Cu/γ-Al_2O_3, (c) Pt-5Cu/γ-Al_2O_3, (d) Pt-10Cu/γ-Al_2O_3, (B): (a) Pt/θ-Al_2O_3, (b) Pt-0.5Cu/θ-Al_2O_3, (c) Pt-5Cu/θ-Al_2O_3, (d) Pt-10Cu/θ-Al_2O_3.

role in the γ phase of Al_2O_3 than in the θ phase. However, CuO peaks appear at 32.5, 35.5, 38.7, 48.7, 53.5, 58.2, 61.5, 66.2, 68.1, 71.7 and 75.3° (JCPDS car no. 48-1548) as shown in Fig. 3 due to the higher surface area of θ-Al_2O_3.

Fig. 4 shows the XRD patterns with reduced Pt-Cu/γ or θ-Al_2O_3 catalysts, and the reduction of catalysts was conducted in hydrogen flow (10 ml/min) at 600 °C for 1 h. The peak was low due to high dispersion of Pt. When the content of copper was increased, the Pt peak was lower gradually. It could be determined that adding copper highly affected the Pt dispersion in γ-Al_2O_3. But Cu_3Pt peak appeared on the surface because of excess added copper in θ-Al_2O_3. Pt peak in θ-Al_2O_3 supported catalyst slightly decreased so that Pt dispersion was increased and the activity could be influenced by formation of Cu_3Pt.

The morphology of the metallic phases and dispersion of Pt in catalysts is revealed by TEM images shown in Fig. 5. In the Pt/γ-Al_2O_3, many black dots regarded as Pt particles are concentrated in the center. But when copper was added on the catalysts, many black dots were spread widely. It means copper makes high dispersion of Pt. In the case of θ-Al_2O_3 supported catalysts, black dots of

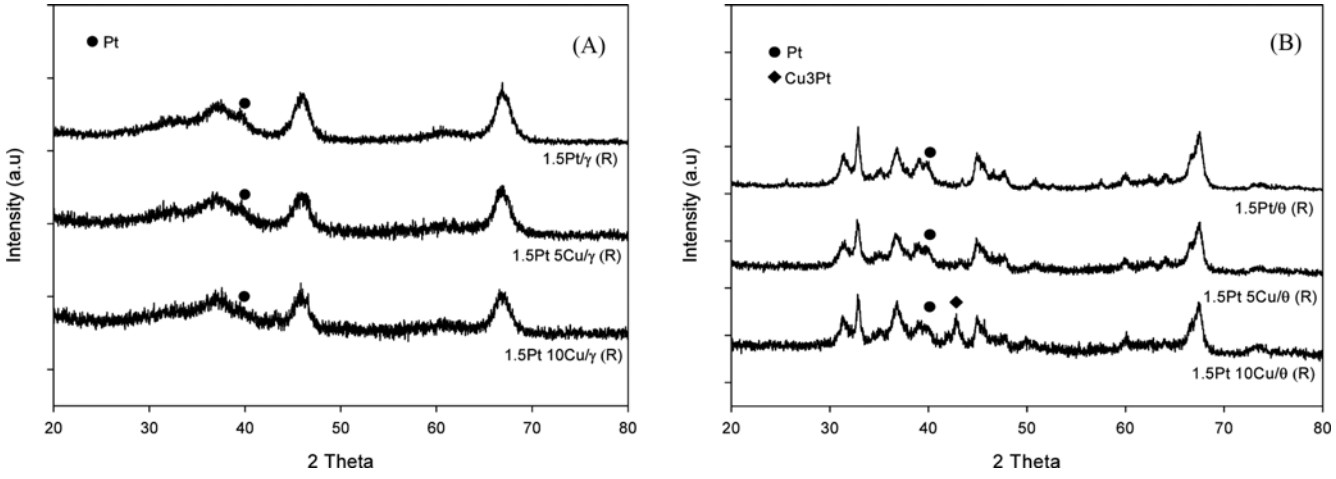

Fig. 4. XRD patterns of (A): (a) Pt/γ-Al_2O_3, (b) Pt-5Cu/γ-Al_2O_3, (c) Pt-10Cu/γ-Al_2O_3, (B): (a) Pt/θ-Al_2O_3, (b) Pt-5Cu/θ-Al_2O_3, (c) Pt-10Cu/θ-Al_2O_3.

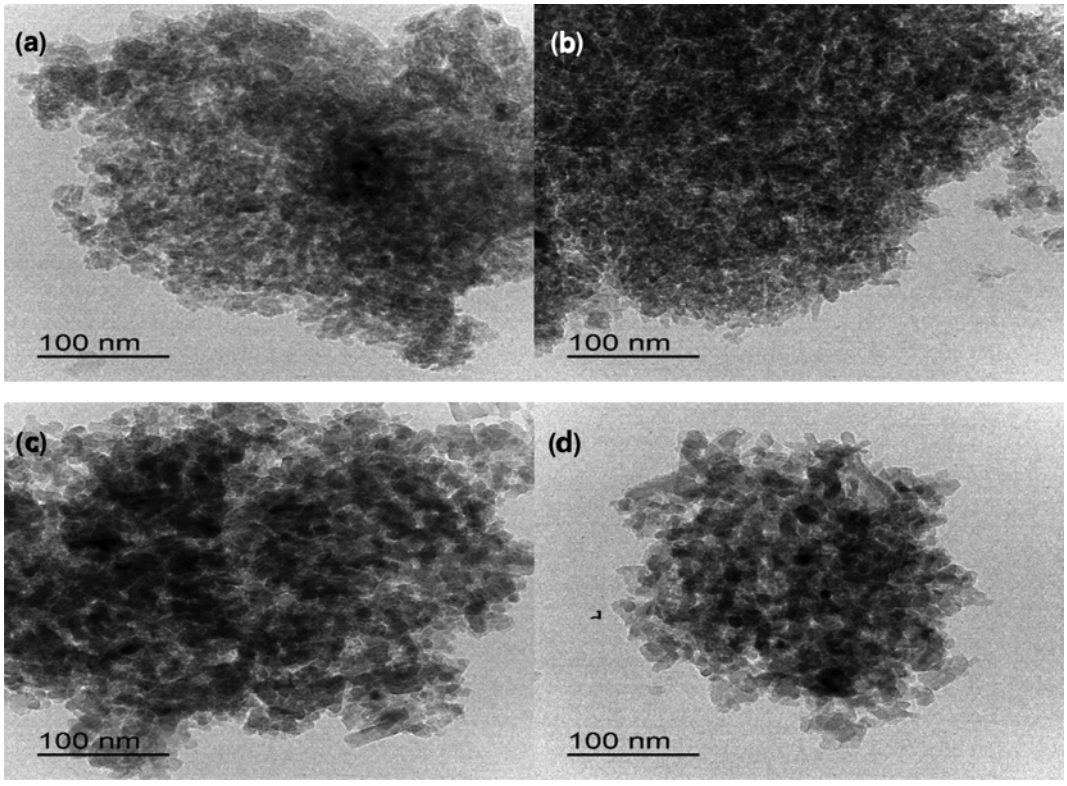

Fig. 5. TEM images of Pt-xCu/γ, θ-Al_2O_3 (a) Pt/γ-Al_2O_3, (b) Pt-5Cu/θ-Al_2O_3, (c) Pt/θ-Al_2O_3, (d) Pt-5Cu/θ-Al_2O_3.

two TEM images are similarly spread compared with γ-Al_2O_3 supported catalysts, which results are similar to XRD analysis.

The dehydrogenation performance of the catalyst is strongly related to the acidity of the catalyst. The effects of copper on the acidity of the Pt/γ and θ-Al_2O_3 catalysts were determined by NH_3-TPD experiments and the corresponding profiles are displayed in Fig. 6. All the NH_3-TPD results were de-convoluted using Lorentzian-Gaussian functions shown in Table 2. The peak at 191-207 °C is attributed as weak acidic sties; the peak at 231-249 °C and 284-314 °C can be assigned at medium acidic sites, and at 340-419 °C can be considered as strong acidic sites. The peaks at 487-700 °C were considered as desorption of the strongly adsorbed water or as de-hydroxylation [24]. The strong acidic sites on Pt/γ-Al_2O_3 (387.2 °C) and Pt/θ-Al_2O_3 (393.6 °C) disappeared after copper addition to Pt/Al_2O_3 catalysts and number of medium acidic sites decreased from 1.4 mmol/g to 0.053 mmol/g at Pt/γ-Al_2O_3 and from 0.77 to 0.066 at Pt/θ-Al_2O_3 with adding Cu. The catalytic yield for propane dehydrogenation to propylene with Pt/γ and θ-Al_2O_3 and Pt-Cu/γ and θ-Al_2O_3 catalyst can be related to the comparatively decreased acidity.

XPS spectra of Pt 4f levels for the Pt-xCu/γ and θ catalysts are shown Figs. 7 and 8. The data shows doublets corresponding to zero valence Pt; Pt $4f_{7/2}$ (ca. 71.3 eV) and Pt $4f_{5/2}$ (ca. 74.6 eV) with a peak separation of 3.3 eV and an area ratio of 1.33 were applied for the fitting procedures. Also, as illustrated by Fig. 7, Pt 4f peak was not observed before reduction. In contrast, the Pt 4f peak appears after reduction treatment and its peak intensity increases with the copper content. As Pt 4f peak of Pt-5Cu/γ-Al_2O_3 is much

Table 2. Acidity profile resulting from NH_3-TPD with Pt-xCu/γ and θ-Al_2O_3 catalysts

Catalyst	Acidic site	Maximum temperature In each peak (°C)	NH_3-Uptake (mmol/g)
Pt/γ-Al_2O_3	Weak	119.4	0.28063
		210.7	0.04538
	Medium	235.5	1.40203
	Strong	387.2	0.13116
	Water	766.5	0.34342
Pt-5Cu/γ-Al_2O_3	Weak	109.5	0.15109
		209.5	1.71364
	Medium	277.9	0.05342
	Water	703	0.43315
Pt/θ-Al_2O_3	Weak	111.4	0.12264
	Medium	231.8	0.77579
	Strong	393.6	0.0427
	Water	704.3	0.21433
Pt-5Cu/θ-Al_2O_3	Weak	143.8	1.3228
	Medium	246.9	0.06597
	Water	642.4	0.1151

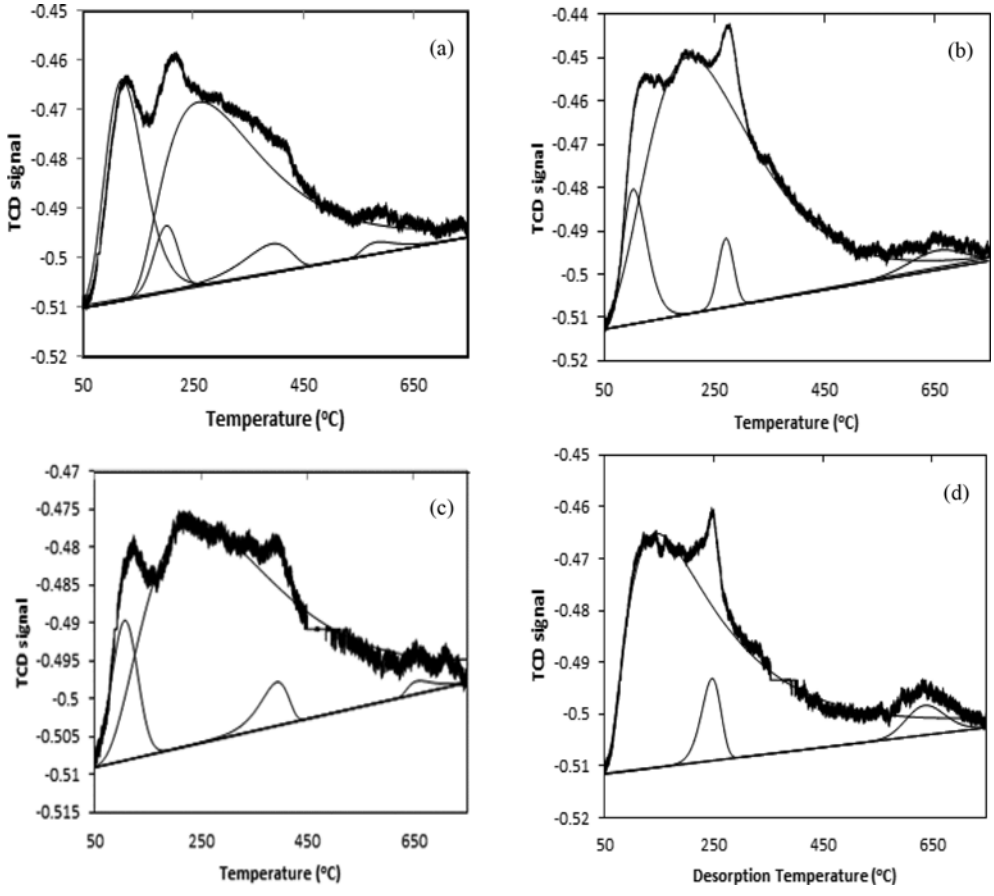

Fig. 6. NH3-TPD spectrum for catalysts as (a) Pt/γ-Al_2O_3 (b) Pt-5Cu/γ-Al_2O_3 (c) Pt/θ-Al_2O_3 (d) Pt-5Cu/θ-Al_2O_3.

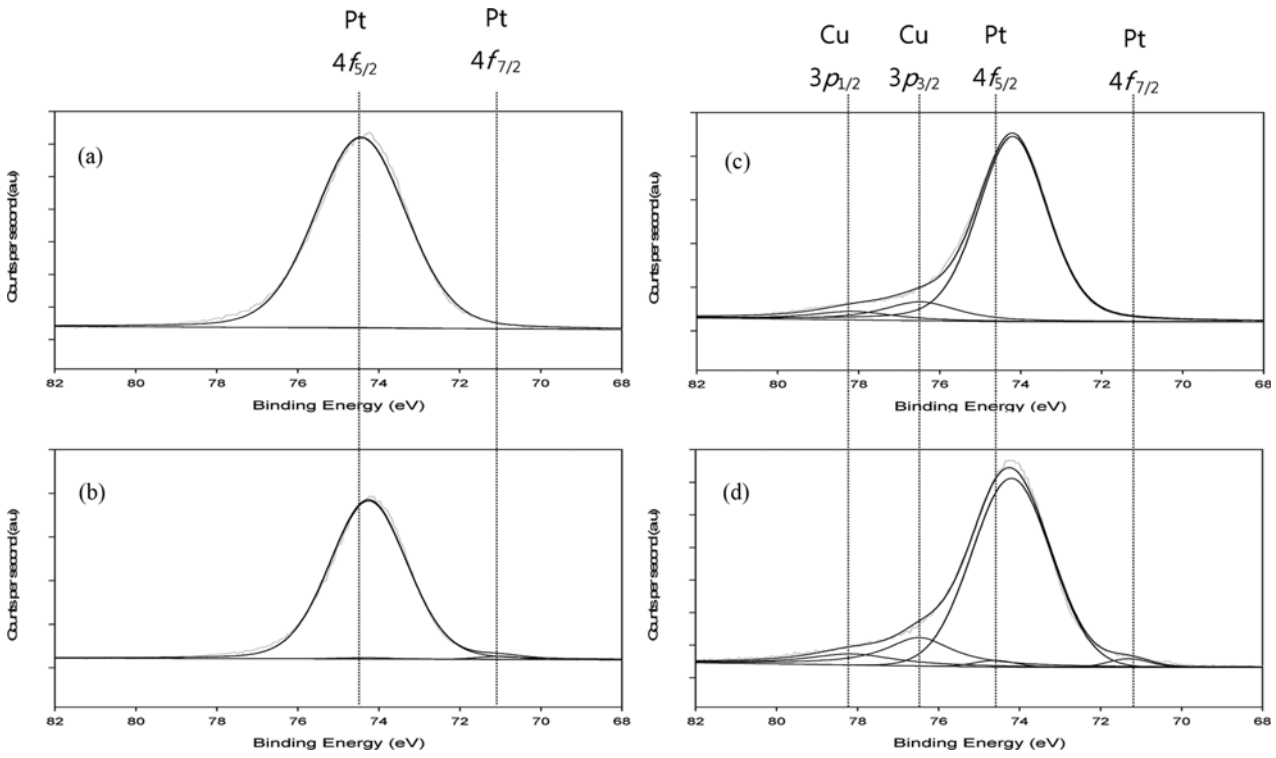

Fig. 7. XPS spectra of Pt 4f four different states: (a) Pt/γ-Al_2O_3 (b) Pt/γ-Al_2O_3 (reduced) (c) Pt-5Cu/γ-Al_2O_3. (d) Pt-5Cu/γ-Al_2O_3 (reduced).

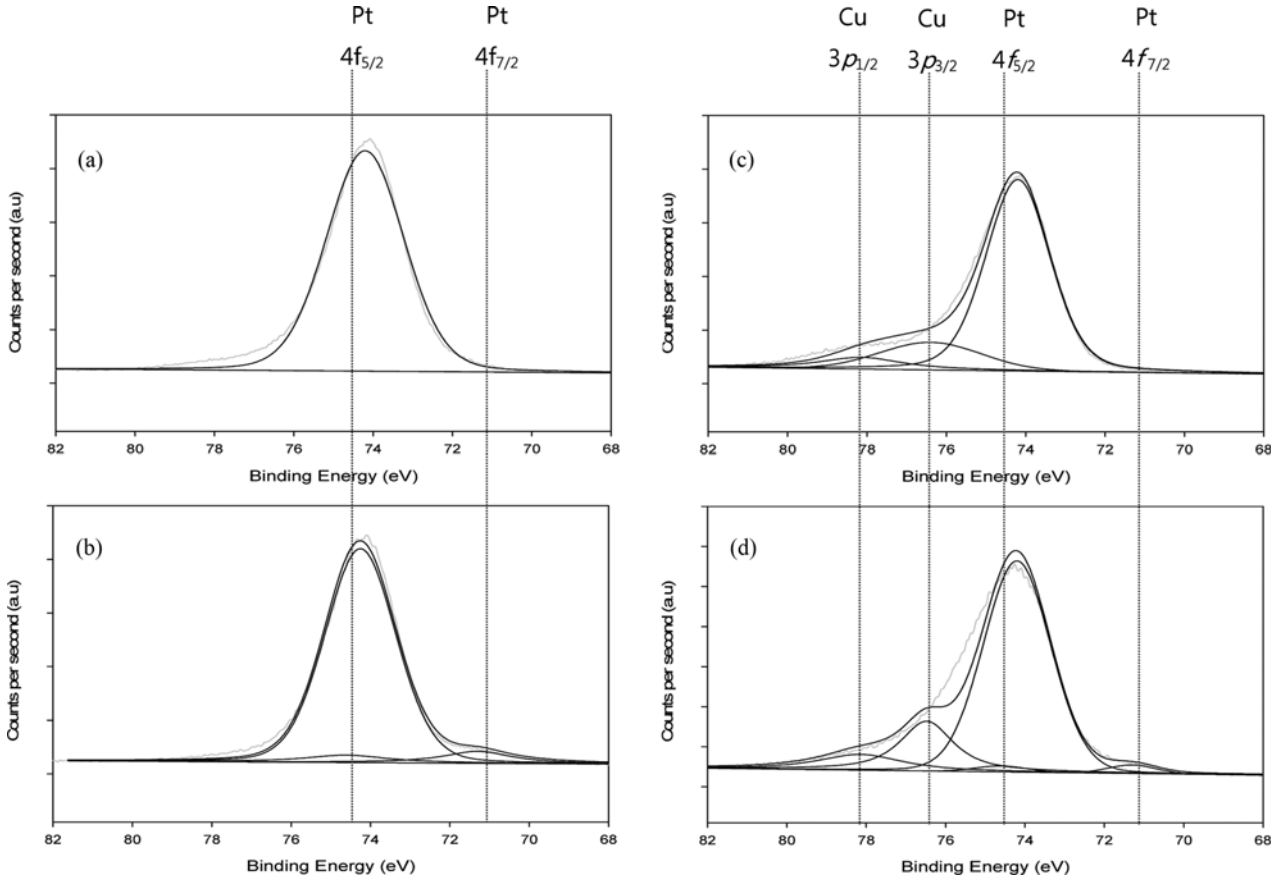

Fig. 8. XPS spectra of Pt 4f four different states: (a) Pt/θ (b) Pt/θ (reduced) (c) Pt-5Cu/θ (d) Pt-5Cu/θ (reduced).

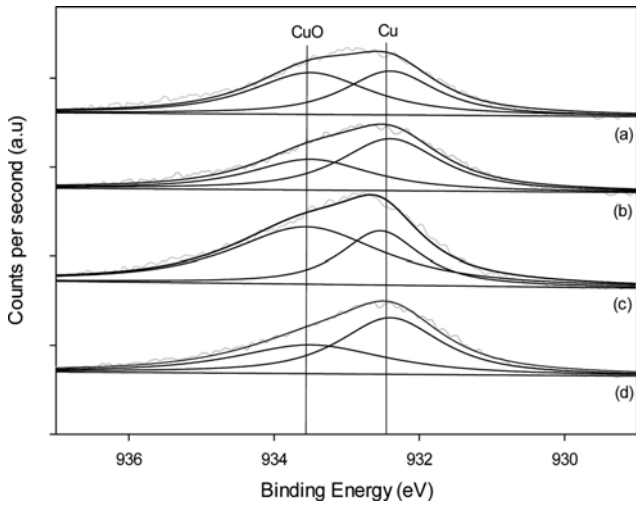

Fig. 9. XPS spectra of CuO and Cu four different states: (a) Pt-5Cu/γ-Al_2O_3 (b) Pt-5Cu/γ-Al_2O_3 (reduced) (c) Pt-5Cu/θ-Al_2O_3 (d) Pt-5Cu/θ-Al_2O_3 (reduced).

larger than Pt/γ-Al_2O_3, in agreement with XRD these results also suggests that the presence of Cu can be related to Pt dispersion. But, there is no distinction between Pt/θ and Pt-5Cu/θ-Al_2O_3 as shown in Fig. 8. It is also the similar result with XRD which has no effect of Pt dispersion with adding Cu in Al_2O_3.

The state of Cu and CuO for the Pt-5Cu/γ and θ was studied by XPS analysis and shown in Fig. 9. These spectra are normalized based on intensity of main peak of Cu $2p_{3/2}$. The Cu $2p_{3/2}$ peak was same as reduced Pt-5Cu/γ and θ catalysts. CuO area ratio compared with Cu is larger in non-reduced catalyst as shown in (a), (c). CuO area was decreased and Cu area was increased after reduction.

2. Catalyst Performance

2-1. Pt-Cu/γ-Al_2O_3 Catalytic Performance for Propane Dehydrogenation

A reaction test was performed to confirm the effect of Cu as a promoter on Pt-Cu/γ and θ-Al_2O_3 catalysts with time on stream. The propane conversions and propylene selectivities are illustrated in Fig. 10. Although initial conversion (5 min) with Pt/γ-Al_2O_3 and Pt-0.5Cu/γ-Al_2O_3 was high due to high activity of platinum, forma-

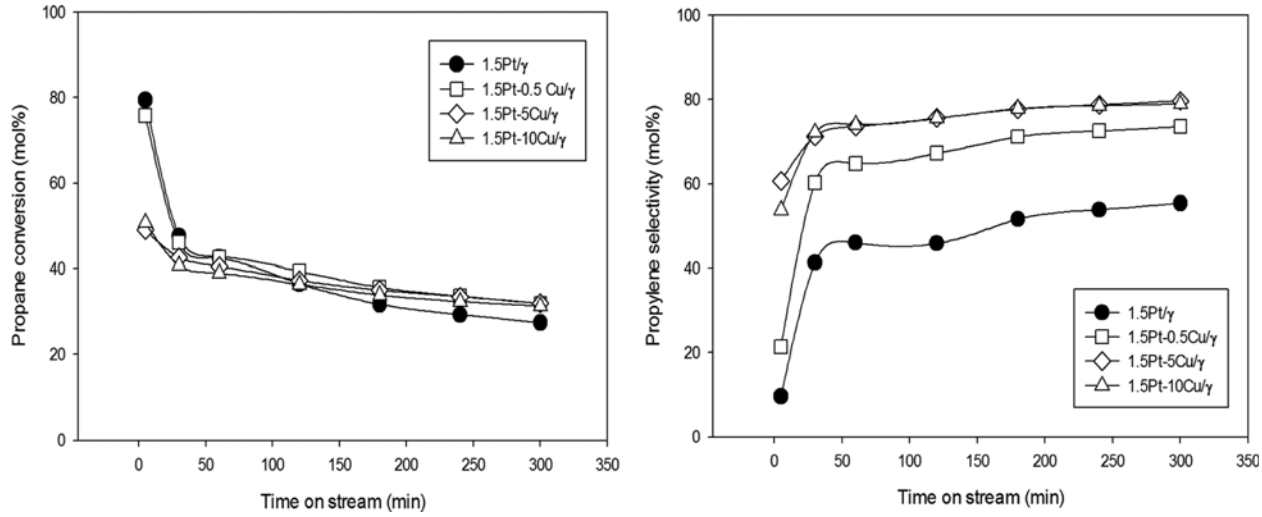

Fig. 10. Conversion and propylene selectivity during 5 h as a function of copper contents in Pt-Cu/γ-Al_2O_3.

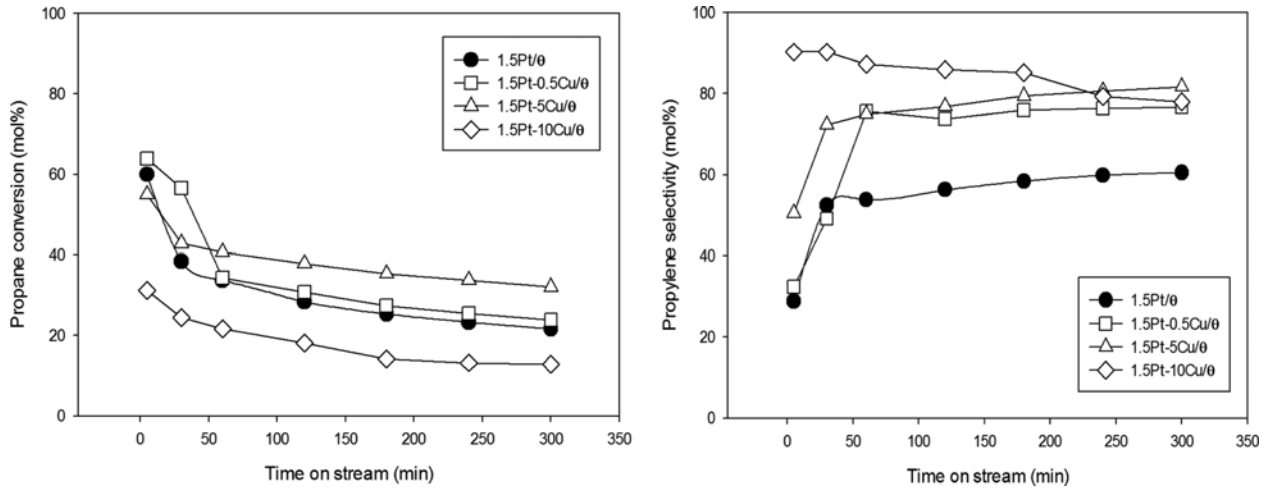

Fig. 11. Conversion and propylene selectivity during 5 h as a function of copper contents in Pt-Cu/θ-Al_2O_3.

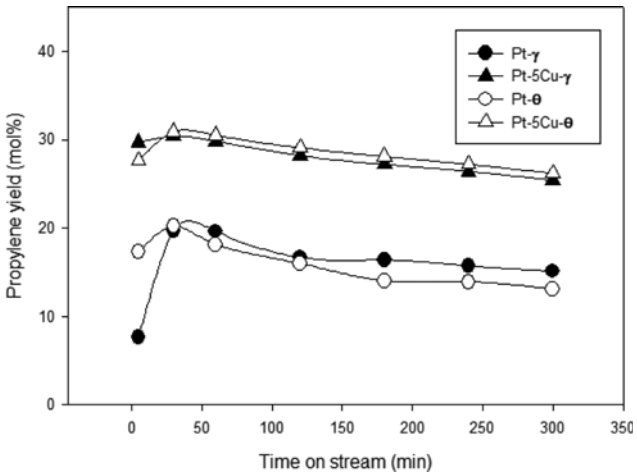

Fig. 12. Propylene yield during 5 h as a function of copper contents and different Al_2O_3 phases in Pt-*x*Cu/γ and θ.

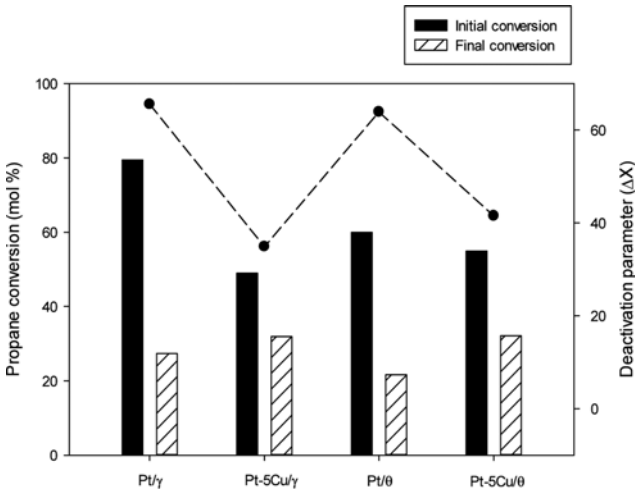

Fig. 13. Deactivation parameter during 5 h as a function of copper addition in Pt-*x*Cu/γ and θ-Al_2O_3.

tion of coke during the reaction caused deactivation of the catalyst. The selectivity showed increasing tendency with enhancing Cu contents, which makes lower acid sites on catalyst surface. However, the effect of Cu content >5 wt% in γ-Al_2O_3 was not observed. It is enough to block all the acid sites on γ-Al_2O_3, when 5 wt% copper is added to Pt/γ-Al_2O_3, so adding copper has no meaning over 5 wt%. And Pt peak in XRD data of 5 wt% and 10 wt% copper on Pt-Cu/γ-Al_2O_3 catalysts has no big difference.

Fig. 11 shows the propane conversion and propylene selectivity on Pt-Cu/θ-Al_2O_3 catalysts compared to γ-Al_2O_3 as the supporter. There are two differences between γ-Al_2O_3 and θ-Al_2O_3. First, adding 0.5 wt% Cu to Pt/θ-Al_2O_3, propane conversion is higher than Pt/θ-Al_2O_3, but this is not the case with γ-Al_2O_3 based catalysts. Secondly, Pt/θ-Al_2O_3 with 10 wt% of Cu has the lowest propane conversion, the highest initial propylene selectivity among the catalysts.

Propylene yields with Pt-*x*Cu/γ and θ-Al_2O_3 catalysts are as shown in Fig. 12. Comparing yield with Pt/γ, θ-Al_2O_3 and Pt-5Cu/γ, θ-Al_2O_3, adding Cu is effective promoter for PDH and irrespective of Al_2O_3 phase. Yield with Pt/γ-Al_2O_3 is a little higher than Pt/θ-Al_2O_3 except initial reaction due to the low selectivity. However, deactivation was prohibited with adding Cu which stabilized the acid site of γ and θ-Al_2O_3. Furthermore, acid suppression effect was attractive in θ-Al_2O_3 more than γ-Al_2O_3, and this result is consistent with NH_3-TPD.

2-2. Deactivation with Pt-Cu/γ-Al_2O_3 Catalyst For Propane Dehydrogenation

Fig. 13 shows the deactivation parameter initial and after 5 h conversion for each Cu content and Al_2O_3 phase in Pt-*x*Cu/γ and θ-Al_2O_3. The deactivation parameter is calculated by dividing the difference between the initial and final conversion. Propane initial conversions of Pt/γ and θ-Al_2O_3 were 79.4% and 60%, respectively. These are higher than the values of initial conversion of 49% and 55% for Pt-5Cu/γ and θ-Al_2O_3, respectively. However, as the reaction progressed, the final conversions of Pt/γ-Al_2O_3, Pt/θ-Al_2O_3, Pt-5Cu/γ-Al_2O_3 and Pt-5Cu/θ-Al_2O_3 were 27.4%, 31.9%, 21.6% and 32.1%, respectively. This indicated that adding copper in Pt/Al_2O_3 can be attributed to block acid sites to improve the catalytic activity of Pt/γ and θ-Al_2O_3 for propane dehydrogenation.

CONCLUSION

We investigated the effect of Pt-*x*Cu/Al_2O_3 with different alumina phases for propane dehydrogenation. Presence of Cu in the Pt/Al_2O_3 catalyst increases its propylene selectivity and yield and decreases the catalyst deactivation rate because adding Cu reduces the number of acid sites and their intensity. The optimized loading content of Cu is 5 wt%. When the copper content was increased, the anti-coking ability of the Pt-Cu/Al_2O_3 catalysts improved and weakened the interaction between coke and catalysts. The cause of deactivation of Pt-10 wt%Cu/θ-Al_2O_3 may be that Cu covered the active site of Pt for formation of Cu_3Pt.

ACKNOWLEDGEMENTS

This work was financed by industry core technology project called Development of high yield propylene production process technology of Ministry of Trade, Industry and Energy (project No.: 100052754-Korea evaluation institute of industrial technology).

REFERENCES

1. G. H. Kim, K. D. Jung, W. I. Kim, B. H. Um, C. H. Shin, K. Oh and H. L. Koh, *Res. Chem. Intermediat.*, **42**, 351 (2016).
2. F. T. Zangeneh, S. Mehrazma and S. Sahebdelfar, *Fuel Process Technol.*, **109**, 118 (2013).
3. S. Sahebdelfar, M. T. Ravanchi, F. Tahriri Zangeneh, S. Mehrazma and S. Rajabi, *Chem. Eng. Res. Des.*, **90**, 1090 (2012).
4. F. T. Zangeneh, S. Sahebdelfar and M. Bahmani., *Chin. J. Chem. Eng.*, **21**, 730 (2013).
5. S. Sahebdelfar and F. T. Zangeneh, *Iran. J. Chem. Eng.*, **7**, 51 (2010).
6. M. Komasi, S. Fatemi and M. Razavian, *Korean J. Chem. Eng.*, **32**, 7 (2015).
7. D. Akporiaye, S. Jensen, U. Olsbye, F. Rohr, E. Rytter, M. Rønnekleiv and A. Spjelkavik, *Ind. Eng. Chem. Res.*, **40**, 4741 (2001).

8. B. K. Vu, M. B. Song, I. Y. Ahn, Y. W. Suh, D. J. Suh, J. S. Kim and E. W. Shin, *J. Ind. Eng. Chem.*, **17**, 71 (2011).
9. Z. Han, S. Li, F. Jiang, T. Wang, X. Ma and J. Gong, *Nanoscale*, **6**, 10000 (2014).
10. V. Mehdi and H. Ali, *Asian J. Chem.*, **22**, 9 (2010).
11. F. T. Zangeneh and S. Sahebdelfar, *Iran. J. Chem. Eng.*, **8**, 49 (2011).
12. C. Yokoyama, S. Bharadwaj and L. Schmidt, *Catal Lett.*, **38**, 181 (1996).
13. S. B. Abd Hamid, D. Lambert and E. G. Derouane, *Catal Today*, **63**, 237 (2000).
14. R. Rioux and M. Vannice, *J. Catal.*, **233**, 147 (2005).
15. J. J. Gao, G. P. Zhou, H. J. Qiu, Y. Wang and J. Wang, *Corros. Sci.*, **108**, 194 (2016).
16. J. Tymoczko, F. Calle-Vallejo, V. Čolić, W. Schuhmann and A. S. Bandarenka, *Electrochim. Acta*, **179**, 469 (2015).
17. A. A. Ensafi, M. M. Abarghoui and B. Rezaei, *Electrochim. Acta*, **190**, 199 (2016).
18. F. Epron, F. Gauthard and J. Barbier, *Appl. Catal., A.*, **237**, 253 (2002).
19. S. Veldurthi, C. H. Shin, O. S. Joo and K. D. Jung, *Catal. Today*, **185**, 88 (2012).
20. C. H. Mauldin and W. C. Baird, US Patent, 4,231,898 (1980).
21. A. Gholidoust, A. Naderifar, M. Rahmani and S. Sahebdelfar, *Int. J. Mod. Phys.: Conference Series*, World Scientific, 168 (2012).
22. C. Casiraghi, A. Ferrari and J. Robertson, *Phys. Rev. B.*, **72**, 085401 (2005).
23. Y. Shan, Z. Sui, Y. Zhu, D. Chen and X. Zhou, *Chem. Eng. J.*, **278**, 240 (2015).
24. B. M. Nagaraja, H. Jung, D. R.Yang and K. D. Jung, *Catal. Today*, **232**, 40 (2014).
25. B. K. Vu, M. B. Song, I. Y. Ahn, Y. W. Suh, D. J. Suh, W. I. Kim, H. L. Koh, Y. G. Choi and E. W. Shin, *Appl. Catal., A.*, **400**, 25 (2011).